Am J Physiol Heart Circ Physiol 291: H2445–H2452, 2006.
First published May 26, 2006; doi:10.1152/ajpheart.00394.2006.

Plasma viscosity regulates systemic and microvascular perfusion during acute extreme anemic conditions

Pedro Cabrales[1] and Amy G. Tsai[1,2]

[1]*La Jolla Bioengineering Institute; and* [2]*Department of Bioengineering, University of California, San Diego, La Jolla, California*

Submitted 14 April 2006; accepted in final form 24 May 2006

Cabrales, Pedro, and Amy G. Tsai. Plasma viscosity regulates systemic and microvascular perfusion during acute extreme anemic conditions. *Am J Physiol Heart Circ Physiol* 291: H2445–H2452, 2006. First published May 26, 2006; doi:10.1152/ajpheart.00394.2006.—The hamster window chamber model was used to study systemic and microvascular hemodynamic responses to extreme hemodilution with low- and high-viscosity plasma expanders (LVPE and HVPE, respectively) to determine whether plasma viscosity is a factor in homeostasis during extreme anemic conditions. Moderated hemodilution was induced by two isovolemic steps performed with 6% 70-kDa dextran until systemic hematocrit (Hct) was reduced to 18% (*level 2*). In a third isovolemic step, hemodilution with LVPE (6% 70-kDa dextran, 2.8 cP) or HVPE (6% 500-kDa dextran, 5.9 cP) reduced Hct to 11%. Systemic parameters, cardiac output (CO), organ flow distribution, microhemodynamics, and functional capillary density, were measured after each exchange dilution. Fluorescent-labeled microspheres were used to measure organ (brain, heart, kidney, liver, lung, and spleen) and window chamber blood flow. Final blood and plasma viscosities after the entire protocol were 2.1 and 1.4 cP, respectively, for LVPE and 2.8 and 2.2 cP, respectively, for HVPE (baseline = 4.2 and 1.2 cP, respectively). HVPE significantly elevated mean arterial pressure and CO compared with LVPE but did not increase vascular resistance. Functional capillary density was significantly higher for HVPE [87% (SD 7) of baseline] than for LVPE [42% (SD 11) of baseline]. Increases in mean arterial blood pressure, CO, and shear stress-mediated factors could be responsible for maintaining organ and microvascular perfusion after exchange with HVPE compared with LVPE. Microhemodynamic data corresponded to microsphere-measured perfusion data in vital organs.

microcirculation; extreme hemodilution; plasma expander; organ flow distribution; intravascular oxygen; functional capillary density

THE PROPER FLUID TO CORRECT a blood loss has been a long-standing subject of debate, particularly in terms of its colligative properties. A key issue in this controversy is the nature of the rheological properties of a plasma expander that ensures adequate vital organ perfusion. Organ blood flow is determined by perfusion pressure, vascular resistance, and blood viscosity. In a rigid tube, changes in apparent fluid viscosity lead to parallel changes in resistance and reciprocal changes in flow according to Poiseuille's equation (2). Conversely, in vivo changes in viscosity may be accompanied by changes in vascular geometry owing to autoregulatory processes driven by changes in production of vasoactive mediators by the endothelium.

Blood viscosity has been shown to be an independent regulator of microvascular blood flow (12, 33, 34, 38). If the circulation behaves as a rigid tube, at constant perfusion pressure, blood flow should increase as blood viscosity is reduced. However, microvascular blood flow is actively regulated in response to change in viscosity as a consequence of the level of shear stress developed in the endothelium. Progressive hemodilution decreases plasma viscosity, whole blood viscosity, and arterial O_2 content, causing the increase in microvascular blood flow. This process reaches a maximum, and continuation of hemodilution beyond this threshold results in vasoconstriction (18) and decreased flow. Our laboratory (7, 38) and others (24, 28, 34) have reported that viscosity and O_2 content play important roles in the microvascular blood flow response to extreme hemodilution, where approximately one-half of the increase in microvascular blood flow is caused by reduced blood viscosity and the remainder by autoregulatory mechanisms related to O_2 content and, possibly, control of shear stress.

Shear stress in the microcirculation has been shown to be regulated within a narrow margin (22) in many studies where portions of the arterial tree were subjected to chronic changes of flow. Several studies have also shown such regulation in arteriolar microcirculation subjected to sudden changes in blood flow (4, 32). Shear stress is a consequence of vascular geometry, flow, and viscosity. Local blood viscosity has been invariably assumed to be constant, although it progressively decreases in the microcirculation due to the Fahraeus-Lindqvist effect (17, 26). Hematocrit (Hct) tends to equalize in the circulation during hemodilution, and use of plasma expanders with different viscosities may significantly affect the acute distribution of shear stress.

Current studies show that if blood viscosity is severely decreased by hemodilution, microvascular function is impaired, and tissue survival is jeopardized as a result of the local microscopic maldistribution of blood flow as well as the deficit in O_2 delivery (38). Clearly, a limit is reached when extreme hemodilution is no longer able to maintain the metabolic needs of the tissue. Nevertheless, microvascular studies in extreme hemodilution show that this limit may be significantly lower than current transfusion triggers, if blood viscosity is partially maintained during hemodilution by an increase in plasma viscosity (10, 11, 38).

Restoration of systemic conditions does not necessarily lead to restoration of microvascular function. However, information on this disparity between systemic and microscopic events is restricted to a few tissues and is seldom available for the vital organs in intact and unanesthetized conditions. The hamster

Address for reprint requests and other correspondence: P. Cabrales, La Jolla Bioengineering Institute, 505 Coast Blvd. South, La Jolla, CA 92037 (e-mail: pcabrales@ucsd.edu).

The costs of publication of this article were defrayed in part by the payment of page charges. The article must therefore be hereby marked "*advertisement*" in accordance with 18 U.S.C. Section 1734 solely to indicate this fact.

chamber window preparation provides a unique opportunity to analyze microcirculation events and establish the relation between observations in the window chamber tissue and other organs. Therefore, the present study was also carried out to determine how perfusion of the window chamber tissue correlates with perfusion in other organs and tissues when the whole organism is subjected to extreme hemodilution with plasma expanders of different viscosities.

The purpose of this study is to test the hypothesis that differences in plasma viscosity in extreme hemodilution may lead to different outcomes in terms of microvascular and systemic regulation. Organ blood flow distribution, cardiac output (CO), and microhemodynamics in the hamster window preparation were measured under conditions of extreme hemodilution (11% Hct) using low- and high-viscosity plasma expanders (LVPE and HVPE).

METHODS

Animal preparation. Male Syrian Golden hamsters (55–65 g body wt; Charles River Laboratories, Boston, MA) were fitted with a dorsal skinfold chamber window. Animal handling and care followed the National Institutes of Health *Guide for the Care and Use of Laboratory Animals*, and the experimental protocol was approved by the local animal care committee. The hamster chamber window model is widely used for microvascular studies in the unanesthetized state; the complete surgical technique is described in detail elsewhere (13, 15). Briefly, the animal was anesthetized with pentobarbital sodium (50 mg/kg ip). After the hair was removed, sutures were used to lift the dorsal skin from the animal, and one frame of the chamber was positioned on the back of the animal. The chamber consists of two identical titanium frames with a 15-mm circular window (12-mm-diameter circular visible field). With the aid of backlighting and a stereomicroscope, one side of the skinfold was removed following the outline of the window until only a thin layer of retractor muscle and the intact subcutaneous skin of the opposing side remained. The cover glass was placed on the exposed skin and held in place by the other frame of the chamber. The intact skin of the other side was exposed to the ambient environment. The animal was allowed ≥2 days for recovery before the preparation was assessed under the microscope for any signs of edema, bleeding, or unusual neovascularization. Animals that were verified to be free of these complications were anesthetized again with pentobarbital sodium. Arterial and venous catheters were implanted in the carotid artery (PE-50) and jugular vein (PE-50), respectively, and filled with a heparinized saline solution (30 IU/ml) to ensure patency at the time of the experiment. Catheters were tunneled under the skin and exteriorized at the dorsal side of the neck, where they were attached to the chamber frame with tape. At 3 to 4 days after the initial surgery, the microvasculature was examined, and only animals that met established systemic and microcirculatory inclusion criteria were entered into the study; animals with low perfusion, inflammation, and edema were excluded (38).

Inclusion criteria. The animals were suitable for the experiments if *1*) systemic parameters were within normal range: heart rate (HR) >340 beats/min, mean arterial blood pressure (MAP) >80 mmHg, systemic Hct >45%, and arterial P_{O_2} (Pa_{O_2}) >50 mmHg, and *2*) microscopic examination of the tissue in the chamber at ×650 magnification showed no signs of edema or bleeding. Hamsters are a fossorial species with a lower Pa_{O_2} than other rodents because of their adaptation to the subterranean environment. However, microvascular P_{O_2} distribution in the chamber window model is the same as in other rodents such as mice (8).

Isovolemic hemodilution protocol. Progressive hemodilution to a final systemic Hct of 11% was accomplished with three isovolemic exchange steps. This protocol is described in detail in our previous reports (6, 10, 38). Briefly, the volume of each exchange-transfusion step was calculated as a percentage of the blood volume, estimated as 7% of body weight. An acute anemic state was induced by lowering systemic Hct to 18% with two steps of progressive isovolemic hemodilution using 6% 70-kDa dextran (Pharmacia) in saline (exchange *levels 1* and *2*). *Level 1* exchange was 40% of blood volume, and *level 2* exchange was 35% of blood volume.

After *level 2* exchange, the animals were randomly divided into two experimental groups according to a sorting scheme based on a list of random numbers (1). Figure 1 illustrates the experimental protocol.

Because mixed blood and dilution material was withdrawn during the exchanges, a 35% blood volume exchange was needed to reduce the functional Hct from 18% to 11% (6, 10, 35, 38, 39). Diluents were filtered (in-line, 0.22-μm filter) and infused into the jugular vein catheter at a rate of 100 μl/min. Blood was simultaneously withdrawn at the same rate from the carotid artery catheter according to a previously established protocol (6, 10, 35, 38, 39). Blood samples were collected at the end of the experiment for subsequent analysis of viscosity and colloid osmotic pressure. The duration of the experiments was 4 h. Each exchange and the respective observation time point after exchange were fully completed in 1 h. Systemic and microcirculation data were collected after a 10-min stabilization period.

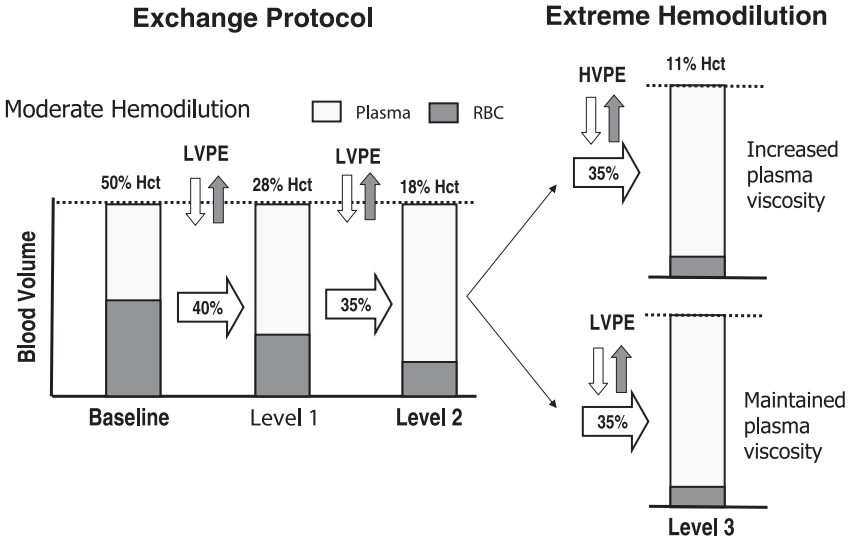

Fig. 1. Hemodilution was attained by means of a progressive, stepwise, isovolemic blood exchange-transfusion protocol in which red blood cell (RBC) volume (gray bar) is continuously decreased and plasma volume is increased (open bar) while total blood volume remains constant (dashed line). Volume of each exchange-transfusion step was calculated as percentage of blood volume, estimated as 7% of body weight. An acute moderate anemic state was induced by lowering systemic Hct by two progressive steps of isovolemic hemodilution (40% and 35% of blood volume) with 6% 70-kDa dextran (viscosity = 2.8 cP, colloid osmotic pressure = 50 mmHg; *levels 1* and *2*). *Level 3* was achieved by a third hemodilution step (35% of blood volume) with use of 6% 70-kDa dextran [low-viscosity plasma expander (LVPE)] or 6% 500-kDa dextran [high-viscosity plasma expander (HVPE), viscosity = 5.9 cP, colloid osmotic pressure = 34 mmHg]. Hemodilution levels are slightly different from volumetric fluid exchanges, because exchanged volume cannot be withdrawn before introduction of diluents.

Systemic parameters. MAP and HR were recorded continuously (model MP 150, Biopac System, Santa Barbara, CA). Hct was measured from centrifuged arterial blood samples collected in heparinized capillary tubes (25 μl, ~50% of the heparinized glass capillary tube was filled). Hb content was determined spectrophotometrically from a single drop of blood (B-Hemoglobin, Hemocue, Stockholm, Sweden).

Blood chemistry and biophysical properties. Arterial blood was collected in heparinized glass capillary tubes (0.05 ml) and immediately analyzed for Pa_{O_2}, arterial P_{CO_2} (Pa_{CO_2}), base excess, and pH with a blood chemistry analyzer (model 248, Bayer, Norwood, MA). The comparatively low Pa_{O_2} and high Pa_{CO_2} of these animals are consequences of their adaptation to a fossorial environment. Blood samples for viscosity and colloid osmotic pressure measurements were quickly withdrawn from the animal with a heparinized 5-ml syringe at the end of the experiment for immediate analysis or refrigerated for next-day analysis. The small size of the animal allowed for withdrawal of only 3 ml of blood after an experiment by exsanguinations over 2 min (unclamping catheter), which was not sufficient for measurement of colloid osmotic pressure, blood viscosity, and plasma viscosity. Viscosity was measured in a cone/plate viscometer (model DV-II Plus, Brookfield Engineering Laboratories, Middleboro, MA) with a cone spindle (model CPE-40) at a shear rate of 160 s^{-1}. Colloid osmotic pressure was measured using a colloid osmometer (model 4420, Wescor, Logan, UT) (40).

Measurement of CO. CO was measured by a modified thermodilution technique (5) in a different group of animals because of the complexity of the setup and the difficulty of positioning the instrumented animal on the microscope. These animals were characterized in terms of systemic parameters to ensure that they presented the same characteristics as those used in the microcirculatory studies. Animals assessed for CO were randomly assigned to different experimental groups. CO was measured 15–20 min after each exchange.

Measurement of blood flow distribution. Fluorescent microspheres (Molecular Probes, Eugene, OR), 15 μm in diameter and four different colors (green, yellow, red, and scarlet), were suspended in saline with 0.02% Tween 80. Microspheres of each color (10^5) were injected 15–20 min after each exchange. Before injection, all fluorescent microspheres were vortexed and mixed in the syringe to obtain a homogenous concentration among the injected volume. The microspheres were injected over 30 s (100 μl). The animals were euthanized with a lethal dose of pentobarbital sodium, and eight vital organs (brain, heart, lung, liver, kidney, spleen, stomach, and intestine) and the window chamber were removed.

For estimation of the number of fluorescent microspheres in each organ, the quantitative relation between the numbers of fluorescent microspheres was determined from the reference blood samples filtered using Perkin-Elmer centrifugal devices (30). Dyes from the retained fluorescent microspheres were eluted with 2 ml of Cellosolve (Aldrich Chemical, Milwaukee, WI), and the fluorescent signals were determined by an automated fluorescent system spectrofluorometer (FluoroMax-2, HORIBA) (30). A calibration standard relating the number of fluorescent microspheres to a given fluorescent signal level was determined for each fluorescent color. The number of fluorescent microspheres in a given volume was determined by 1:10 dilution in a hemocytometer chamber (repeated 9 times). This relation was determined for each fluorescent color, and the 95% confidence interval about this value was estimated (29).

Traditionally, the numbers of microspheres lodging in organ pieces have been used to estimate the blood flow distribution in organs. Regions of high flow have more microspheres than regions of low flow. Microspheres lodge in organ regions in proportion to the amount of blood flow to that region (16, 31). However, because microspheres are discrete particles, there is noise in their distribution. Smaller organ regions have fewer microspheres and, hence, greater counting noise. At least 300 microspheres must be trapped in the reference sample and organs to ensure validity of the measurements (21).

Functional capillary density. Functional capillaries are defined as capillary segments through which at least a single red blood cell (RBC) flows in a 30- to 45-s period. Ten successive microscopic fields were assessed, totaling a region of 0.46 mm^2. Each field had between two and five capillary segments with RBC flow. For evaluation of functional capillary density (FCD, cm^{-1}), i.e., total length of RBC-perfused capillaries divided by the area of the microscopic field of view, the length of capillaries through which RBCs flowed in the field of view was measured and added. The relative change in FCD from baseline levels after each intervention indicates the extent of capillary perfusion (9, 37).

Microhemodynamics. Arteriolar and venular blood flow velocities were measured on-line by the photodiode cross-correlation method (19) with a photodiode/velocity tracker (model 102B, Vista Electronics, San Diego, CA). The measured centerline velocity (V) was corrected according to vessel size to obtain the mean RBC velocity (27). A video image-shearing method was used to measure vessel diameter (D) (20). Blood flow ($\dot{Q}$) was calculated from the measured values as follows: $\dot{Q} = \pi \times V \times (D/2)^2$. Changes in arteriolar and venular diameter from baseline were used as indicators of a change in vascular tone. This calculation assumes a parabolic velocity profile and has been found to be applicable to 15- to 80-μm-ID tubes and for 6–60% Hct (27). Wall shear stress (WSS) was defined as follows: $WSS = WSR \times \eta$, where WSR is the wall shear rate ($8V \times D^{-1}$) and η is the microvascular blood viscosity or plasma viscosity.

Organ O_2 supply. O_2 supply is calculated as follows

$$O_2 \text{ supply} = Hb_{blood} \times Sa_{O_2}\% \times Q_{organ} \times CO$$

where Hb_{blood} is Hb in blood (g/dl), $Sa_{O_2}\%$ is arteriolar O_2 saturation, $\dot{Q}_{organ}$ is the flow fraction for an organ, and CO is cardiac output.

Experimental setup. The unanesthetized animal was placed in a restraining tube with a longitudinal slit from which the window chamber protruded and then fixed to the stage of a transillumination intravital microscope (model BX51WI, Olympus, New Hyde Park, NY). The tissue image was projected onto a charge-coupled device camera (COHU 4815) connected to a videocassette recorder and viewed on a monitor. The animals were allowed 20 min to adjust to the change in the tube environment before measurements were carried out using a ×40 (LUMPFL-WIR, 0.8 NA, Olympus) water-immersion objective. The same sites of study were followed throughout the experiment, so that comparisons could be made directly with baseline levels.

Data analysis. Values are means (SD). Data within each group were analyzed using repeated-measures ANOVA (Kruskal-Wallis test). When appropriate, post hoc analyses were performed with Dunn's multiple-comparison test. Different groups of animals were compared with the Mann-Whitney rank-sum test (Prism 4.01, GraphPad, San Diego, CA). Microhemodynamic measurements were compared with baseline levels obtained before the experimental procedure. Microhemodynamic data are presented as absolute values and ratios relative to baseline values. A ratio of 1.0 signifies no change from baseline; lower and higher ratios indicate changes proportionally lower and higher than baseline (i.e., 1.5 would mean a 50% increase from baseline). The same vessels and functional capillary fields were followed, so that direct comparisons with their baseline levels could be performed, allowing for more robust statistics for small sample populations. Pearson's product-moment correlation was used to test linear correlation between microvascular flows and organ blood flow. Changes were considered statistically significant if $P < 0.05$.

RESULTS

All 24 of the animals tolerated the entire hemodilution protocol without visible signs of discomfort. The animals were assigned randomly to experimental groups as follows: LVPE hemodilution with 6% 70-kDa dextran ($n = 12$, with 6 animals

Table 1. *Laboratory parameters before and after blood exchange*

		Moderate Hemodilution		Extreme Hemodilution	
	Baseline (n = 12)	*Level 1* (n = 12)	*Level 2* (n = 12)	*Level 3* LVPE (n = 6)	*Level 3* HVPE (n = 6)
Hct, %	49.1 (1.7)	29.1 (1.9)*	18.3 (1.4)*	11.1 (0.8)*	11.6 (0.7)*
Hb, g/dl	14.7 (0.5)	9.4 (0.6)*	5.9 (0.7)*	3.8 (0.5)*	3.9 (0.4)*
MAP, mmHg	111.2 (5.9)	96.2 (8.8)*	88.2 (6.8)*	77.1 (5.9)*	86.9 (6.3)*†
HR, beats/min	434 (33)	447 (41)	471 (42)	415 (42)	453 (38)
Pa_{O_2}, mmHg	57.9 (5.8)	67.8 (9.8)	88.0 (11.2)*	107.2 (12.6)*	96.6 (8.4)*
Pa_{CO_2}, mmHg	53.4 (5.0)	54.9 (6.4)	46.8 (6.0)*	37.5 (6.8)*	43.1 (6.6)*
pH_a	7.35 (0.02)	7.35 (0.02)	7.37 (0.02)	7.33 (0.03)	7.36 (0.02)
BE, mmol/l	3.8 (1.4)	3.1 (2.0)	2.1 (2.0)	−2.7 (1.8)*	0.8 (1.6)*†

Values are means (SD). Baseline includes all animals in the study. LVPE, low-viscosity plasma expander; HVPE, high-viscosity plasma expander. Hct, systemic hematocrit; Hb, hemoglobin content of blood; MAP, mean arterial blood pressure; HR, heart rate; CO, cardiac output; Pa_{O_2}, arterial P_{O_2}; Pa_{CO_2}, arterial P_{CO_2}; pH_a, arterial pH; BE, base excess. *$P < 0.05$ vs. baseline. †$P < 0.05$ vs. LVPE.

used for CO measurements) and HVPE hemodilution with 6% 500-kDa dextran (n = 12, with 6 animals used for CO measurements). Microhemodynamics of animals used for CO measurements were not studied (see METHODS), but systemic parameters paralleled those of the animals used for microvascular study. Six additional animals, which were not subjected to hemodilution, were used to characterize baseline blood organ flow distributions and CO.

The baseline data set is a combination of data from all experimental groups. *Level 1* and *2* data sets are combinations of data from the two experimental groups in the hemodilution protocol. One-way ANOVA on these data showed no significant differences in systemic or microcirculatory parameters. Therefore, data could be combined into representative groups for each of the three states: baseline, *level 1*, and *level 2*.

Systemic and microvascular hemodynamic results paralleled those obtained in a previous study during identical hemodilution conditions (10, 36, 38). Briefly, moderate hemodilution to *level 2* with 70-kDa dextran to 18.1% Hct reduced MAP to 88.2 mmHg (SD 6.8) [from 111.2 mmHg (SD 5.9)], increased Pa_{O_2} and Pa_{CO_2}, and increased microvascular flow. Detailed systemic and blood laboratory parameters before and after hemodilution are presented in Table 1. CO increased as hemodilution progressed, indicating a significant lowering of vascular resistance at *level 2*. Specific systemic hemodynamic changes before and after hemodilution are presented in Table 2. Microvascular flow was significantly increased. FCD was reduced to 92% (SD 5) of baseline after *level 1* exchange and significantly reduced to 87% (SD 7) after *level 2* exchange.

The difference between LVPE and HVPE was studied after the third hemodilution step to *level 3*, where blood viscosities were 2.1 cP (SD 0.2) and 2.8 cP (SD 0.3), respectively. After hemodilution, colloid osmotic pressure in the LVPE [17 mmHg (SD 2)] and HVPE [16 mmHg (SD 2)] groups was not different from that in nonhemodiluted animals [17 mmHg (SD 1)]. This difference in viscosities led to a significantly lower MAP than baseline and among groups: 77.1 mmHg (SD 5.9) for LVPE and 86.9 mmHg (SD 6.3) for HVPE, respectively. CO was significantly lowered from baseline for LVPE and was significantly elevated for HVPE compared with LVPE (Table 3). CO and MAP data were used to calculate peripheral vascular resistance and vascular hindrance. As mentioned above, vascular resistance decreased during acute hemodilution (*levels 1* and *2*) and returned to baseline values after *level 3* with LVPE or HVPE. Vascular hindrance, which accounts for the geometric contribution to resistance, was significantly decreased from baseline after *level 3* with LVPE and was maintained with HVPE.

Consistent with previous findings, microvascular flow was increased above baseline for HVPE in arterioles and venules and significantly lower than baseline for LVPE (Fig. 2). The difference in flow between LVPE and HVPE was significant for arterioles and venules ($P < 0.05$). FCD was lower from *level 2* for LVPE [42% (SD 11) of baseline] and maintained for HVPE [73% (SD 9) of baseline] and statistically greater than LVPE (Fig. 3). Vessel wall shear rate was maintained after *level 3* for LVPE and HVPE, and calculated wall shear stress was statistically increased for HVPE compared LVPE (Fig. 4).

Blood flow distribution to the different organs and calculated organ blood flows are presented in Table 3. *Level 1* hemodilution showed a decrease in flow that was significant in the lung ($P < 0.05$) and the brain ($P < 0.10$). The significant decrease in lung flow may be a consequence of self-regulation. The heart, liver, lung, and window chamber tissue showed a

Table 2. *CO and vascular resistance*

		Moderate Hemodilution		Extreme Hemodilution	
	Baseline (n = 12)	*Level 1* (n = 12)	*Level 2* (n = 12)	*Level 3* LVPE (n = 6)	*Level 3* HVPE (n = 6)
Hct, %	50.4 (2.1)	27.8 (1.9)*	18.3 (1.5)*	10.1 (0.9)*	10.3 (1.2)*
Hb, g/dl	16.2 (1.2)	9.4 (0.6)*	6.0 (0.8)*	3.7 (0.5)*	3.7 (0.7)*
CO, ml/min	17.9 (3.3)	24.3 (4.3)*	26.8 (4.9)*	14.2 (3.0)*	19.6 (2.6)†
CI, ml·min/kg	203 (18)	277 (48)*	309 (57)*	170 (39)*	215 (19)
VR, dyn·s·cm^{-5}	0.47 (0.18)	0.34 (0.12)*	0.29 (0.14)*	0.40 (0.11)	0.36 (0.10)
VH, 1/cm^3	112 (43)			190 (52)*	128 (39)†

Values are means (SD). CO, cardiac output; CI, cardiac index; VR, vascular resistance; VH, vascular hindrance. *$P < 0.05$ vs. baseline. †$P < 0.05$ vs. LVPE.

Table 3. *Organ flow distribution*

Organ (Tissue)	Baseline	Moderate Hemodilution		Extreme Hemodilution	
		Level 1	*Level 2*	*Level 3* LVPE	*Level 3* HVPE
Brain	2.37 (0.69) [0.13 (0.05)]	2.50 (0.50)	3.67 (0.92)*	1.92 (0.52)*	2.63 (0.72)†
Heart	1.59 (0.28) [0.10 (0.04)]	2.88 (1.16)*	3.25 (1.79)*	1.06 (0.45)	2.17 (0.49)*‡
Kidney	4.78 (1.42) [0.27 (0.08)]	7.97 (2.32)*	10.3 (2.74)*	4.56 (1.07)	5.36 (1.09)†
Liver	1.77 (0.41) [0.09 (0.04)]	2.76 (0.92)*	3.64 (1.12)*	1.67 (0.51)	3.22 (1.32)*‡
Lung	1.44 (0.43) [0.08 (0.02)]	0.93 (0.17)*	1.94 (0.54)*	0.81 (0.32)*	2.02 (0.51)*†‡
Spleen	0.91 (0.15) [0.04 (0.01)]	1.28 (0.28)	1.27 (0.27)	0.62 (0.23)*	0.99 (0.21)†
Window	0.66 (0.28) [0.03 (0.01)]	0.69 (0.27)	1.16 (0.39)*	0.28 (0.12)*	0.89 (0.14)†‡

Values are means (SD) in ml/min; fraction of injected microphases is shown in brackets. Baseline include all animals in the study. *$P < 0.05$; †$P < 0.10$ vs. baseline; ‡$P < 0.05$ vs. LVPE.

significant increase in flow for HVPE compared with LVPE ($P < 0.05$). Correlation between microvascular flow and flow to the brain ($R^2 = 0.89$), heart ($R^2 = 0.70$), liver ($R^2 = 0.80$), and lungs ($R^2 = 0.71$) was statistically significant ($P < 0.05$).

O_2 supply to the different organs (Fig. 5) was calculated using data on organ blood flow distribution, Hb, Pa_{O_2}, and CO. Regulation of O_2 supply was observed during moderate hemodilution (*levels 1* and *2*), and the decrease in O_2-carrying capacity (Hct) was compensated by the increase in flow. Notably, the heart, kidney, liver, and window chamber tissue maintained their O_2 supply. Changes in organ O_2 supply at *level 3* for LVPE and HVPE were, in general, less than half of baseline. Consistent with the increases in CO at identical Hct, HVPE always provided a better O_2 supply than LVPE.

DISCUSSION

The principal finding of the present study is that, in extreme hemodilution, the hemodynamic outcome produced by HVPE (6% 500-kDa dextran, 5.9 cP) was superior to that produced by an identical degree of dilution with LVPE (6% 70-kDa dextran, 2.8 cP). Hemodynamics were assessed in terms of MAP, CO, and organ flow distribution. The effects on microvascular hemodynamics were comparable to those previously reported in a similar protocol and show that maintaining blood rheological properties during hemodilution by increasing plasma viscosity (by means of HVPE) is of direct benefit in increasing microvascular flow (38), sustaining capillary pressure, maintaining FCD (10), boosting production of endothelium-mediated factors (36), and enhancing organ flow compared with a conventional LVPE.

In previous work in the area of microcirculatory effects of plasma viscosity during extreme hemodilution, it was assumed that hemodynamic and metabolic events in the microcirculation of preparations such as the chamber window model reflect systemic responses. This assumption is, in general, confirmed by the present findings. Heart perfusion during increased

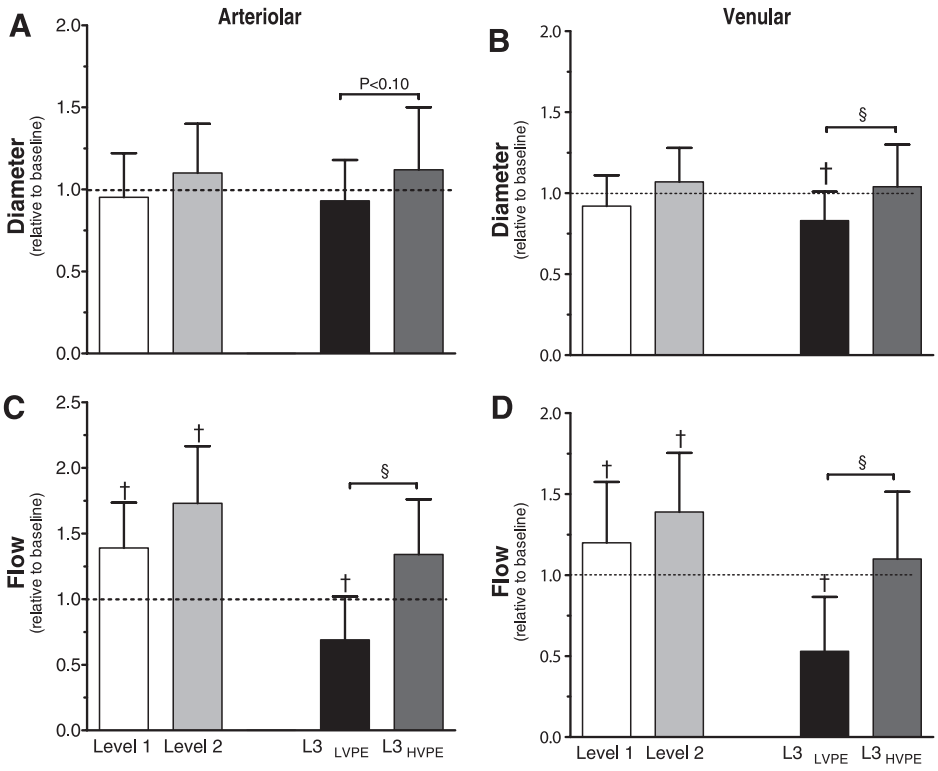

Fig. 2. Relative changes in baseline arteriolar and venular hemodynamics for *level 1*, *level 2*, *level 3* LVPE and HVPE ($L3_{LVPE}$ and $L3_{HVPE}$). Dashed line, baseline. †$P < 0.05$ vs. baseline. §$P < 0.05$ among groups. Diameters (μm) are as follows: 57.7 (SD 7.1) for arterioles ($n = 48$) and 60.1 (SD 8.2) for venules ($n = 50$) at baseline, 56.4 (SD 8.2) for arterioles and 59.5 (SD 8.3) for venules at *level 1*, 60.5 (SD 9.6) for arterioles and 63.0 (SD 7.9) for venules at *level 2*, 54.8 (SD 11.0) for arterioles ($n = 24$) and 55.8 (SD 8.4) for venules ($n = 25$) at $L3_{LVPE}$, and 64.2 (SD 10.2) for arterioles ($n = 24$) and 62.2 (SD 6.9) for venules ($n = 25$) at $L3_{HVPE}$ (n is number of vessels). RBC velocities (mm/s) are as follows: 4.4 (SD 1.2) for arterioles and 2.6 (SD 0.8) for venules at baseline, 6.6 (SD 1.9) for arterioles and 3.6 (SD 1.3) for venules at *level 1*, 6.8 (SD 1.5) for arterioles and 3.4 (SD 1.1) for venules at *level 2*, 3.6 (SD 1.3) for arterioles and 1.5 (SD 0.7) for venules at $L3_{LVPE}$, and 4.5 (SD 1.2) for arterioles and 1.9 (SD 1.3) for venules at $L3_{HVPE}$. Calculated flows (nl/s) are as follows: 12.8 (SD 2.9) for arterioles and 6.7 (SD 2.5) for venules at baseline, 6.7 (SD 1.6) for arterioles and 3.2 (SD 1.1) for venules at *level 1*, 19.3 (SD 7.8) for arterioles and 9.8 (SD 4.6) for venules at *level 2*, 9.7 (SD 3.8) for arterioles and 3.0 (SD 2.1) for venules at $L3_{LVPE}$, and 16.8 (SD 8.6) for arterioles and 6.6 (SD 3.3) for venules at $L3_{HVPE}$.

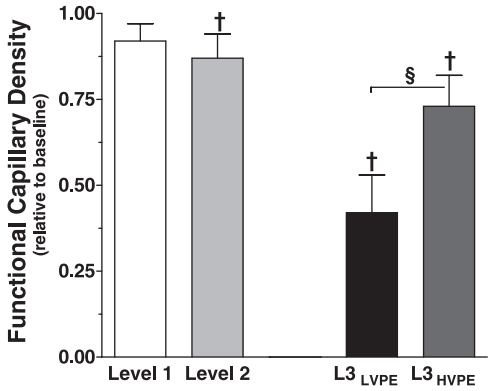

Fig. 3. Effects of plasma viscosity on capillary perfusion during hemodilution. Functional capillary density (FCD) was unchanged after *level 1* exchange. Drop in FCD was greater with $L3_{LVPE}$ than with $L3_{HVPE}$. Values are means (SD). FCD values (cm^{-1}) are as follows: 115 (SD 18) at baseline, 108 (SD 20) at *level 1*, 96 (SD 14) at *level 2*, 41 (SD 12) at $L3_{LVPE}$, and 81 (SD 14) at $L3_{HVPE}$. †$P < 0.05$ vs. baseline. §$P < 0.05$ among groups.

plasma viscosity (HVPE) was higher than baseline in the heart ($P < 0.05$) and ($P < 0.10$) window chamber and also higher ($P < 0.05$) than with LVPE (Table 3). In general, these results show an impairment of perfusion when blood viscosity is significantly reduced (LVPE), particularly in the brain, lung, spleen, and window chamber, which is, in part, reflected in the blood laboratory parameters and microvascular observations. Overall, the tissue in the window chamber underestimates improvements of perfusion due to high plasma viscosity and overestimates the deficits in perfusion compared with other tissues and organs.

Calculation of the O_2 supply to organs and tissues shows that extreme hemodilution could be associated with an important O_2 deficit. Hemodynamic advantages of HVPE over LVPE were evident in the heart, liver, lung, and window chamber tissue. The remainder of the tissues tested (brain, kidney, and spleen) showed a similar tendency. Nevertheless, changes were not statistically significant. In most instances, increased plasma viscosity (HVPE) during extreme hemodilution appears to ensure the O_2 supply at a minimum of one-third of baseline with almost one-fifth of O_2-carrying capacity. Additionally, improved gas exchange and oxygenation are supported by a positive acid-base balance during increased viscosity compared with a negative balance at the lower plasma viscosity. Thus HVPE should result in more sustainability of extreme dilution over time.

The availability of microvascular and systemic hemodynamic data allows more definitive conclusions on mechanisms that differentiate outcomes between LVPE and HVPE during hemodilution. Vascular hindrance at 11% Hct was significantly increased for LVPE relative to baseline, indicating probable vasoconstriction. This vascular tone effect was evident and significant in the venules of the window chamber. Therefore, the increased vascular tone with LVPE may account for the consistent trend toward lower perfusion in the different organs than with HVPE, as shown by arteriolar and venular flow in the window chamber.

The change in plasma viscosity also modifies whole blood viscosity; therefore, it is difficult to separate the respective roles of these viscosities in systemic and microvascular flow responses. However, the effects of plasma viscosity manipulation on microhemodynamic conditions were similar to results

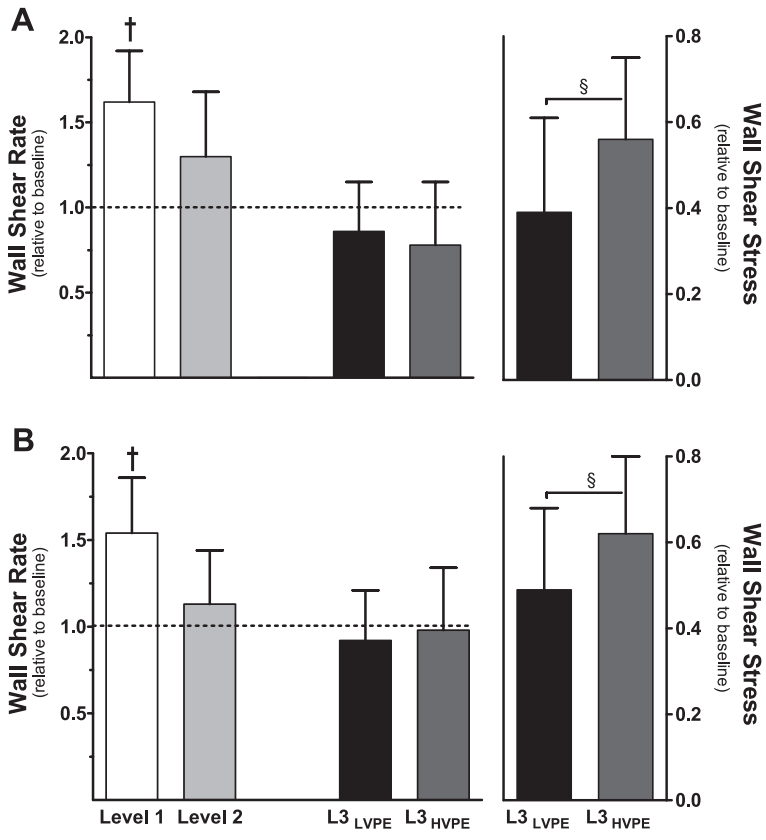

Fig. 4. Wall shear stress and wall shear rate after *level 3* hemodilution with LVPE and HVPE. Hemodilution with LVPE reduced arteriolar and venular wall shear stress to 40% (SD 19) and 49% (SD 22) of baseline, respectively. Hemodilution with HVPE maintained arteriolar and venular wall shear rate, and wall shear stress was 43% and 27% higher, respectively, than with LVPE. †$P < 0.05$. Wall shear stress values (dyn/cm^2) are as follows: 4.8 (SD 0.9) for arterioles and 0.9 (SD 0.2) for venules at $L3_{LVPE}$ and 5.8 (SD 1.6) for arterioles and 1.5 (SD 0.4) for venules at $L3_{HVPE}$. †$P < 0.05$ vs. baseline. §$P < 0.05$ among groups.

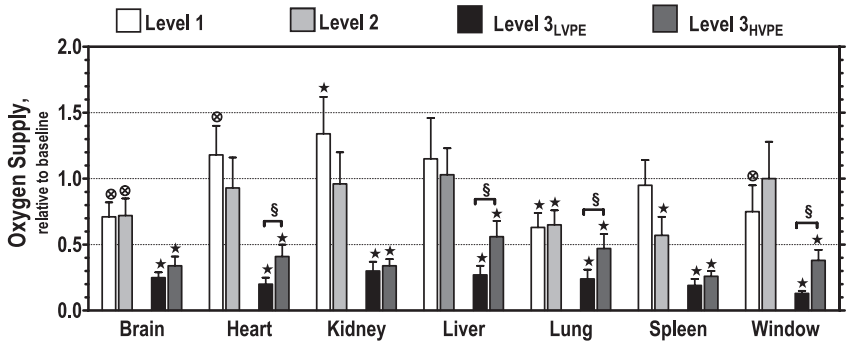

Fig. 5. Organ O_2 supply. Regional differences in circulatory responses during hemodilution may not be adequately reflected by measurements of global O_2 delivery and oxygenation status in individual tissues and organs. $\star P < 0.05$, $\otimes P < 0.10$ vs. baseline. $\S P < 0.05$ among groups.

reported for an identical hemodilution protocol using nonfunctional RBCs, in which viscosity, but not O_2-carrying capacity, was maintained (7). The importance of plasma viscosity in the regulation of flow is not surprising. Because of the axial migration of RBCs in flowing blood, plasma is the principal interface with the blood vessel wall (3). Shear stress exerted by the plasma moving near the endothelial surface influences vessel diameter and modulates the release of autacoids (prostacyclin and nitric oxide). In a previous study using the same model and protocol, Tsai et al. (36) showed that increased shear stress was associated with an increase in the measured concentration of perivascular nitric oxide, with concomitant vasodilator effects. Another possibility is that the viscous drag exerted by large polymers is sensed via the glycocalyx, triggering the activation of endothelial mechanisms (14). Nonselective channels activated by stretching the cell membrane, as well as inwardly rectifying K^+ channels activated by fluid shear stress, have been described in cell culture (23, 25). Hyperpolarization due to the opening of Ca^{2+}-activated K^+ channels is part of the endothelial response to enhanced plasma viscosity.

The present study shows that these microvascular effects evidenced in the window chamber are indicative of related and similar effects in the microcirculation of the brain, heart, liver, and lungs, because these tissues show similar changes in perfusion when subjected to extreme hemodilution with HVPE and LVPE. The statistical significance of the correlation coefficients relating changes supports the hypothesis of the commonality of autoregulatory effects and responses to changes in blood and plasma viscosity between these organs and the window chamber model. Therefore, the combination of vasodilation and increased flow due to HVPE should lead to increased capillary pressure and, therefore, increased FCD, as demonstrated by Cabrales et al. (10), in the microcirculation of the tested organs.

Changes in hemodynamics and respiration affect the energy expenditure of the heart (product of MAP and CO): 44,100, 51,900, 52,500, 24,300, and 37,800 erg/s for baseline, *level 1*, *level 2*, LVPE, and HVPE, respectively. The increase in energy expenditure by the heart after moderated hemodilution was followed by the drop to one-half of baseline with LVPE and a return to baseline with HVPE. Heart perfusion and O_2 delivery decreased with LVPE compared with HVPE, which explains the decrease of cardiac performance. O_2 delivered by coronary arteries is extracted during one passage through the myocardial vessels. Thus the supply of O_2 to the myocardial cells is flow limited, and the reduction in heart flow curtails O_2 delivery, because the extraction of O_2 is nearly maximal, even under basal conditions.

Moderate hemodilution increased left ventricular stroke volume (LVSV = cardiac index ÷ HR) from 0.48 ml/kg at baseline to 0.62 and 0.65 ml/kg at *levels 1* and *2*, respectively. Changes in LVSV could be explained by the decrease in vascular resistance, increase in perfusion, and maintenance of O_2 supply. Extreme hemodilution to 11% Hct with LVPE prevented the increase of stroke volume (0.40 ml/kg), whereas stroke volume returned to near baseline values (0.48 ml/kg) with HVPE. Differences in heart function after extreme hemodilution with LVPE can therefore be attributed to the increased vascular resistance, decreased heart perfusion, and severely decreased heart O_2 supply.

In conclusion, augmentation of plasma viscosity to maintain blood rheological properties is beneficial during extreme hemodilution compared with significant lowering of blood viscosity with an LVPE. Improvement of microvascular function, particularly capillary perfusion, compensated for the potentially negative effect of increasing peripheral vascular resistance by increasing plasma and blood viscosity. Maintenance of normal physiological conditions for the whole organism after the increase of plasma viscosity was evidenced by a sustained and increased perfusion to vital organs when intrinsic blood O_2-carrying capacity was decreased to an extreme (11% Hct). Conversely, this effect was not attainable by lowering whole blood viscosity by decreasing Hct without raising plasma viscosity. These phenomena appear to be directly related to the increase in shear stress and decrease in vascular resistance consequent to an increase in plasma viscosity, leading to vasodilation and improved transmission of central pressure to organs and their microcirculation, which maintain FCD. These findings also support the hypothesis that results deduced from findings in the hamster chamber window model, which allows the observation and quantitative characterization of the microcirculation in the intact, unanesthetized state, are representative of events in some of the major organs that are not accessible by microvascular techniques. The O_2 supply attained in extreme hemodilution, even in the optimal conditions resulting from induction of a high plasma viscosity, are below the threshold of safety that determines the need for a blood transfusion; however, the maintenance of microvascular function well beyond this threshold indicates that increasing plasma viscosity is a mechanism for providing an extra margin of safety before blood transfusion is required.

ACKNOWLEDGMENTS

The authors thank Leo Bondar for processing the organs and Froilan P. Barra and Cynthia Walser for surgical preparation of the animals.

GRANTS

This work was supported by Bioengineering Research Partnership Grant R24-HL-64395 and Grants R01-HL-62354, R01-HL-62318, and R01-HL-76182 from the National Heart, Lung, and Blood Institute.

REFERENCES

1. **Altman DG and Bland JM.** Statistics notes: how to randomise. *BMJ* 319: 703–704, 1999.
2. **Anderson SM, Rich GF, Roos C, Lee LP, and Lee JS.** Fluid restitution and blood volume redistribution in anesthetized rabbits in response to vasoactive drugs. *Circulation* 90: 509–514, 1994.
3. **Bayliss LE.** The axial drift of the red cells when blood flows in a narrow tube. *J Physiol* 149: 593–613, 1959.
4. **Bohlen HG.** Mechanism of increased vessel wall nitric oxide concentrations during intestinal absorption. *Am J Physiol Heart Circ Physiol* 275: H542–H550, 1998.
5. **Cabrales P, Acero C, Intaglietta M, and Tsai AG.** Measurement of the cardiac output in small animals by thermodilution. *Microvasc Res* 66: 77–82, 2003.
6. **Cabrales P, Kanika ND, Manjula BN, Tsai AG, Acharya SA, and Intaglietta M.** Microvascular P_{O_2} during extreme hemodilution with hemoglobin site specifically pegylated at Cys-93(β) in hamster window chamber. *Am J Physiol Heart Circ Physiol* 287: H1609–H1617, 2004.
7. **Cabrales P, Martini J, Intaglietta M, and Tsai AG.** Blood viscosity maintains microvascular conditions during normovolemic anemia independent of blood oxygen-carrying capacity. *Am J Physiol Heart Circ Physiol* 291: H581–H590, 2006.
8. **Cabrales P, Tsai AG, Frangos JA, and Intaglietta M.** Role of endothelial nitric oxide in microvascular oxygen delivery and consumption. *Free Radic Biol Med* 39: 1229–1237, 2005.
9. **Cabrales P, Tsai AG, and Intaglietta M.** Increased tissue P_{O_2} and decreased O_2 delivery and consumption after 80% exchange transfusion with polymerized hemoglobin. *Am J Physiol Heart Circ Physiol* 287: H2825–H2833, 2004.
10. **Cabrales P, Tsai AG, and Intaglietta M.** Microvascular pressure and functional capillary density in extreme hemodilution with low- and high-viscosity dextran and a low-viscosity Hb-based O_2 carrier. *Am J Physiol Heart Circ Physiol* 287: H363–H373, 2004.
11. **Cabrales P, Tsai AG, Winslow RM, and Intaglietta M.** Effects of extreme hemodilution with hemoglobin-based O_2 carriers on microvascular pressure. *Am J Physiol Heart Circ Physiol* 288: H2146–H2153, 2005.
12. **Chen RY, Carlin RD, Simchon S, Jan KM, and Chien S.** Effects of dextran-induced hyperviscosity on regional blood flow and hemodynamics in dogs. *Am J Physiol Heart Circ Physiol* 256: H898–H905, 1989.
13. **Colantuoni A, Bertuglia S, and Intaglietta M.** Quantitation of rhythmic diameter changes in arterial microcirculation. *Am J Physiol Heart Circ Physiol* 246: H508–H517, 1984.
14. **Cooke JP, Rossitch E Jr, Andon NA, Loscalzo J, and Dzau VJ.** Flow activates an endothelial potassium channel to release an endogenous nitrovasodilator. *J Clin Invest* 88: 1663–1671, 1991.
15. **Endrich B, Asaishi K, Götz A, and Messmer K.** A new chamber technique for microvascular studies in unanaesthetized hamsters. *Res Exp Med (Berl)* 177: 125–134, 1980.
16. **Heymann MA, Payne BD, Hoffman JI, and Rudolph AM.** Blood flow measurements with radionuclide-labeled particles. *Prog Cardiovasc Dis* 20: 55–79, 1977.
17. **House SD and Lipowsky HH.** Microvascular hematocrit and red cell flux in rat cremaster muscle. *Am J Physiol Heart Circ Physiol* 252: H211–H222, 1987.
18. **Hudak ML, Jones MD Jr, Popel AS, Koehler RC, Traystman RJ, and Zeger SL.** Hemodilution causes size-dependent constriction of pial arterioles in the cat. *Am J Physiol Heart Circ Physiol* 257: H912–H917, 1989.
19. **Intaglietta M, Silverman NR, and Tompkins WR.** Capillary flow velocity measurements in vivo and in situ by television methods. *Microvasc Res* 10: 165–179, 1975.
20. **Intaglietta M and Tompkins WR.** Microvascular measurements by video image shearing and splitting. *Microvasc Res* 5: 309–312, 1973.
21. **Ishise S, Pegram BL, Yamamoto J, Kitamura Y, and Frohlich ED.** Reference sample microsphere method: cardiac output and blood flows in conscious rat. *Am J Physiol Heart Circ Physiol* 239: H443–H449, 1980.
22. **Kassab GS and Fung YC.** The pattern of coronary arteriolar bifurcations and the uniform shear hypothesis. *Ann Biomed Eng* 23: 13–20, 1995.
23. **Kohler R, Schonfelder G, Hopp H, Distler A, and Hoyer J.** Stretch-activated cation channel in human umbilical vein endothelium in normal pregnancy and in preeclampsia. *J Hypertens* 16: 1149–1156, 1998.
24. **Krieter H, Bruckner UB, Kefalianakis F, and Messmer K.** Does colloid-induced plasma hyperviscosity in haemodilution jeopardize perfusion and oxygenation of vital organs? *Acta Anaesthesiol Scand* 39: 236–244, 1995.
25. **Lansman JB, Hallam TJ, and Rink TJ.** Single stretch-activated ion channels in vascular endothelial cells as mechanotransducers? *Nature* 325: 811–813, 1987.
26. **Lipowsky HH and Firrell JC.** Microvascular hemodynamics during systemic hemodilution and hemoconcentration. *Am J Physiol Heart Circ Physiol* 250: H908–H922, 1986.
27. **Lipowsky HH and Zweifach BW.** Application of the "two-slit" photometric technique to the measurement of microvascular volumetric flow rates. *Microvasc Res* 15: 93–101, 1978.
28. **Menu P, Longrois D, Faivre B, Donner M, Labrude P, Stoltz JF, and Vigneron C.** Rheological behaviour of red blood cells suspended in hemoglobin solutions. In vitro study comparing dextran-benzene-tetracarboxylate hemoglobin, stroma free hemoglobin and plasma expanders. *Transfusion Sci* 20: 5–16, 1999.
29. **Mood AM, Graybill FA, and Boes DC.** *Introduction to the Theory of Statistics*. New York: McGraw-Hill, 1974.
30. **Raab S, Thein E, Harris AG, and Messmer K.** A new sample-processing unit for the fluorescent microsphere method. *Am J Physiol Heart Circ Physiol* 276: H1801–H1806, 1999.
31. **Schimmel C, Frazer D, Huckins SR, and Glenny RW.** Validation of automated spectrofluorometry for measurement of regional organ perfusion using fluorescent microspheres. *Comput Methods Programs Biomed* 62: 115–125, 2000.
32. **Smiesko V and Johnson PC.** The arterial lumen is controlled by flow-related shear stress. *News Physiol Sci* 8: 34–38, 1993.
33. **Tomiyama Y, Brian JE Jr, and Todd MM.** Plasma viscosity and cerebral blood flow. *Am J Physiol Heart Circ Physiol* 279: H1949–H1954, 2000.
34. **Tomiyama Y, Jansen K, Brian JE Jr, and Todd MM.** Hemodilution, cerebral O_2 delivery, and cerebral blood flow: a study using hyperbaric oxygenation. *Am J Physiol Heart Circ Physiol* 276: H1190–H1196, 1999.
35. **Tsai AG.** Influence of cell-free hemoglobin on local tissue perfusion and oxygenation after acute anemia after isovolemic hemodilution. *Transfusion* 41: 1290–1298, 2001.
36. **Tsai AG, Acero C, Nance PR, Cabrales P, Frangos JA, Buerk DG, and Intaglietta M.** Elevated plasma viscosity in extreme hemodilution increases perivascular nitric oxide concentration and microvascular perfusion. *Am J Physiol Heart Circ Physiol* 288: H1730–H1739, 2005.
37. **Tsai AG, Cabrales P, Winslow RM, and Intaglietta M.** Microvascular oxygen distribution in awake hamster window chamber model during hyperoxia. *Am J Physiol Heart Circ Physiol* 285: H1537–H1545, 2003.
38. **Tsai AG, Friesenecker B, McCarthy M, Sakai H, and Intaglietta M.** Plasma viscosity regulates capillary perfusion during extreme hemodilution in hamster skinfold model. *Am J Physiol Heart Circ Physiol* 275: H2170–H2180, 1998.
39. **Tsai AG, Vandegriff KD, Intaglietta M, and Winslow RM.** Targeted O_2 delivery by low-P_{50} hemoglobin: a new basis for O_2 therapeutics. *Am J Physiol Heart Circ Physiol* 285: H1411–H1419, 2003.
40. **Webb AR, Barclay SA, and Bennett ED.** In vitro colloid osmotic pressure of commonly used plasma expanders and substitutes: a study of the diffusibility of colloid molecules. *Intensive Care Med* 15: 116–120, 1989.